Talanta 169 (2017) 163–169

Contents lists available at ScienceDirect

Talanta

journal homepage: www.elsevier.com/locate/talanta

A sensitive and disposable indium tin oxide based electrochemical immunosensor for label-free detection of MAGE-1

Burçak Demirbakan[a,*], Mustafa Kemal Sezgintürk[b]

[a] Namık Kemal University, Faculty of Science, Chemistry Department, Biochemistry Division, Tekirdağ, Turkey
[b] Çanakkale Eighteen March University, Faculty of Engineering, Bioengineering Department, Çanakkale, Turkey

ARTICLE INFO

Keywords:
3-Glycidoxypropyltrimethoxysilane (3-GOPS)
MAGE-1
Regeneration
Square wave voltammetry (SWV)
Electrochemical impedance spectroscopy (EIS)

ABSTRACT

MAGE-1 (MAGE, for melanoma antigen), was identified by virtue of its processing and cell surface expression as a tumor-specific peptide bound to major histocompatibility complexes which was reactive with autolytic T cells. 3-Glycidoxypropyltrimethoxysilane (3-GOPS) is frequently employed for the preparation of dense heterometal hybrid polymers which are used, e.g., for hard coatings of organic polymers and contact lens materials in the optical industry.

In this study, we have improved a new immunological biosensor with indium tin oxide (ITO). Then, Anti-MAGE-1 antibody was covalently immobilized with 3-GOPS which formed a self-assembled monolayers (SAMs) on modified ITO electrodes. Analytical characteristics such as square wave voltammetry, linear determination range, repeatability, reproducibility and regeneration of biosensors are determined. All characterization steps are monitored by electrochemical impedance spectroscopy (EIS), cyclic voltammetry (CV).

The developed biosensor has wide determination range (0.5 fg–15 fg/mL). To investigate long shelf life of the fabricated biosensor, the immunosensors were stored at 4 °C for periods ten weeks. Futhermore, binding kinetics of MAGE1 to antiMAGE-1 is monitored by single frequency technique in real time. Additionally, Kramer's-Kronig transform was used to understand whether the impedance spectra of biosensor system are affected from the variation that occurred because of external factor. Morphological characteristics of constructed biosensor were observed by scanning electron microscopy. Real human serum samples were also analyzed by the proposed biosensor, successfully. A commercial ELISA kit was also used as a reference method to validate the results obtained by the biosensor.

Finally, this biosensor was tried in real blood sample and that showed it could be utilized in clinical applications. This biosensor can be preferred due to it has a wide linear range and it can be prepared easily.

1. Introduction

Melanoma-associated antigens (MAGE) were firstly found as tumor-associated antigens in melanoma patients [1] but now clear that these proteins involve a super-family of more than 60 genes in humans [4,5]. The MAGEs are severed into two groups, MAGE-I (MAGE-A, MAGE-B and MAGE-C) [2,3] and MAGE-II (MAGE-D, MAGE-E, MAGE-F, MAGE-H, MAGE-L and NDN) [2,3], based on the chromosomal locations of the genes and the distribution of their products [4,5]. MAGE-II are ecumenically expressed in normal tissues and cancer cells [6,7]. MAGE-I genes expression is limited to a little number of normal tissues such as placenta, certain stages of embryonic development [6,7]. MAGE-I proteins are members of family of Cancer Testis Antigens (CTA) [8]. CTAs, are expressed in a amplitude of tumors while expression in normal tissues is limited to immunoprivileged sites such as the testis and placenta. MAGE genes are the best known members of the CTA family [9]. CTAs are serviced on the cell surface by MHC-II molecules and identified by cytotoxic T lymphocytes (CTLs). Thus, this is a proper target molecule of CTL specific immune therapy [10,11]. MAGE family is a wide gene family which contains more than sixty members, some of which code tumor specific antigens that have large expression in several tumors such as melanoma, breast cancer, lung cancer, pancreatic cancer and some urological malignancies [34–38].

3-Glycidoxypropyltrimethoxysilane (3-GOPS) is frequently employed for the preparation of dense heterometal hybrid polymers which are used, e.g., for hard coatings of organic polymers and contact lens materials in the optical industry [12]. 3-GOPS is an ideal agent in bio-applications [13–15], besides, it is very practical silane modification agent that glycidoxy compound containing epoxy group. The electrode

* Corresponding author.
E-mail addresses: burcak_demirbakan@hotmail.com (B. Demirbakan), msezginturk@comu.edu.tr (M.K. Sezgintürk).

http://dx.doi.org/10.1016/j.talanta.2017.03.076
Received 18 December 2016; Received in revised form 20 March 2017; Accepted 25 March 2017
Available online 29 March 2017

surface covalently covered with the silane agent can be used to assemble hydroxyl-, thiol- or amine- including groups [29], depending on the pH of the reaction. Hereby, 3-GOPS can be used to bound metallic surfaces including –OH groups. 3-GOPS has been to generate a high-density polyethylene glycol (PEG) surface on glass slide for use in arrays [28]. Moreover, it has been used in the development of a high-throughput analyzer using biochip technology on aluminum oxide sheets [27] and in the activation of glass surfaces for determination of antibodies specific for hepatitis B and C viruses [26].

In the present work, 3-GOPS solution was used as a self-assembled monolayer (SAM) material to react with hydroxyl groups. The SAMs material has epoxy groups and high chemical activity of these groups allows the simple relevance mechanisms of the specific ligands [13–16].

Lately, significant attempts have been intended to enhance the disposable analytical devices with easy, conducting property and great sensing ability, such as indium tin oxide polyethylene terephthalate (ITO-PET) [17,18], pencil graphite based electrode [19,20] and graphite paper based electrode [21,22]. ITO has a good electrical conductivity and also it is transparent conductive electrode [23]. ITO has many advantages. Some of those are low cost, high sensitivity, large surface area and good conductivity [24].

In the aimed study, a sensitive and regenerative electrochemical immunosensor was prepared by 3-GOPS solution that was used as SAMs on indium tin oxide surface. In each step of constructed immunosensor was characterized by EIS, CV and SWV methods. Moreover SEM images of the immunosensor were taken. In the present work, one of the most important points was -single frequency technique- that was used to observe the interaction between MAGE-I antigen and MAGE-I antibody. Thanks to the technique can be possible to control the biosensor with a total time and a repeat time [25]. The other important point was regeneration of the immunosensor. Although using working electrode was disposable it could be regenerated. This property of the electrode was good advantage for lower cost of this study. The proposed immunosensor has wide detection range and the concentrations of MAGE-I as low as pg mL^{-1}. The convincing results of real human serum samples indication further demonstrated that the ITO based immunosensor has encouraging perspectives in the field of electroanalysis.

2. Experimental

2.1. Materials and instrumentations

3-GOPS solution, anti-MAGE-1, MAGE-1 antigen and ITO-PET films (the transmittance is 550 nm (> 79%) and surface resistivity is 60 Ω/square) were procured from Sigma Aldrich (St. Louris, MO, USA). Commercial ELISA kits were bought from LSBio LifeSpan Biosciences, Inc. MAGE-1 and anti-MAGE-1 portions, 0.5% bovine serum albumin (BSA) solution, human serum portions were confected at the determined concentrations and were kept at –20 °C until use. All the supplementary chemicals were prepared with ultra pure water (18.2 MΩ deionized). All electrochemical measurements were performed on a Gamry Reference 600 Potentiostat/Galvanostat (Gamry Instruments, Warminster, USA) electrochemical workstation. To be able to view morphology of the different surfaces in the proposed biosensor was used to scanning electron microscopy (FEI-Quanta FEG 250) at the Scientific and Technological Research Center of Namık Kemal University (NABILTEM). The phosphate buffer solutions (PBS, pH 7.0) were prepared from 1 M KCl, KH_2PO_4 and K2HPO4 compounds. A three-electrode cell with a sheet of ITO substrate working electrode, having 2 mm×20 mm size, Ag/AgCl (3 M KCl) reference electrode and a platinum wire auxiliary electrode were used in the voltammetric and amperometric measurements.

2.2. Preparation of the modified electrode

Prior to the modification of 3-GOPS agent that the self-assembled monolayer material, ITO surface was cleaned by sonicated in acetone, soap solution and ultra pure water for 10 min, respectively. After this work, to form –OH groups onto the surface, each of the cleaned electrodes were immersed in hydroxyl solution, containing of NH4OH solution, H_2O_2 solution and ultra pure water (1:1:5 v/v), and the electrodes were incubated for 90 min at 25 °C. After this incubation period, the electrodes were carefully washed with deionised water and dried by argon gas.

2.3. Fabrication of the impedimetric biosensor

After the cleaning proses and the forming hydroxyl group on the electrode surface, ITO electrodes were carefully immersed into 1.5% 3-GOPS solution (in pure toluene) and were incubated in the darkness for 16 h. After this step, the SAM-modified electrodes were washed with toluene solution and ultra pure water respectively and immediately afterwards dried in a stream of pure argon gas. The anti-MAGE-1 antibody was then covalently immobilized on the activated SAMs layer from 100 μL solution (11 ng/mL) by 30 min incubation in a dark medium. Hereupon, the electrodes were washed by ultra pure water and then dried in a stream of pure argon gas carefully. Lastly, the electrodes were incubated with solution of BSA (0.5%) that blocking agent for 1 h. The overall period of the biosensor fabrication was also submitted in Scheme 1.

2.4. Electrochemical characterization

Electrochemical impedance, cyclic voltammetry and square wave voltammetry measurements were used to detect ITO electrode modification and immobilization processes. These measurements (EIS and CV) were recorded at certain frequency range (0.05–10.000 Hz), a 20 mV voltage and SWV (potential range: 0–1.2 V, pulse size: 25 mV and frequency: 25 Hz) applying in a freshly prepared containing 5 mM potassium hexacyanoferrate(III), 5 mM potassium hexacyanoferrate(II) $K_3[Fe(CN)_6]/K_4[Fe(CN)_6]$ (1:1) and 50 mM phosphate buffer solution (PBS) (pH 7.0). The SWV was also used to confirm the validity of the data obtained from the Nyquist diagram compared to other techniques (EIS and CV). The charge in Rct relative to the reference surface was used as the output signal.

3. Result and discussion

3.1. Immobilization of the anti-MAGE-1 immunosensor

Immobilization steps play a major role in terms of characteristics of the proposed biosensor, hence, all steps were implemented with $K_3[Fe(CN)_6]/K_4[Fe(CN)_6]$ redox couple which ensures the rapid electron transfer of bioactive species to the electrode surface. The electrochemical characterization of the anti-MAGE-1 biosensor was examined with EIS spectra and CV voltammograms (Fig. 1).

The EIS graph has two parts, the real part (Z′) versus imaginary part (Z′′) displaying the Rct on the electrode surface as identical to the diameter of the semicircle on the Nyquist plot, and can be used to identify features at the interface of the electrode [30]. While the semicircle part observed at high frequencies is related to the electron transfer limited process of $Fe(CN)_6^{3-/4-}$, the linear part is diffusion dependent. The diameter of the semicircle is used to calculate the Rct value on any electrode surface. As seen in Fig. 1C, an equivalent circuit can be modeled for the measured EIS data. This equivalent circuit model consists of ohmic resistance (Rs), Warburg impedance (Zw) and Rct data [25]. These data belong to the resistance of the electrolyte solution between the indium tin oxide electrode and the reference electrode. Rs and Zw data are not affected by the immobilization of

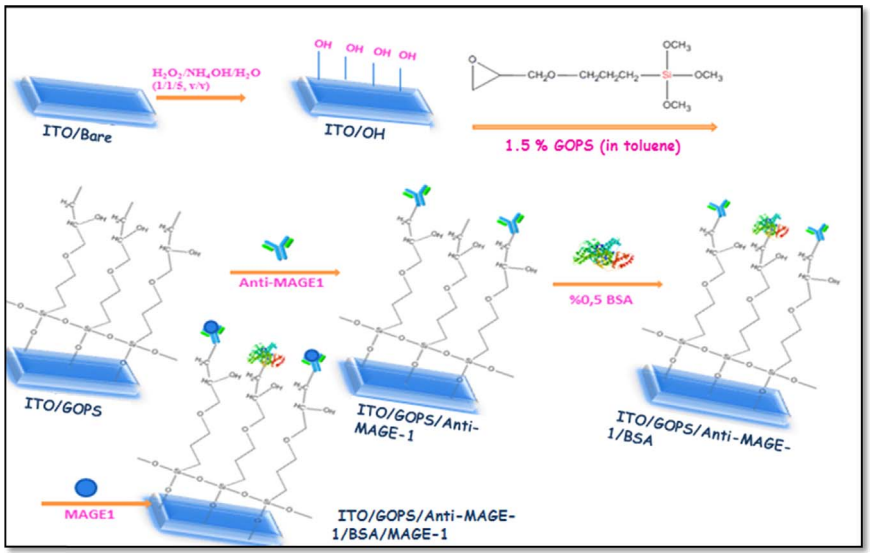

Scheme 1. All immobilization steps belonging to the proposed biosensor.

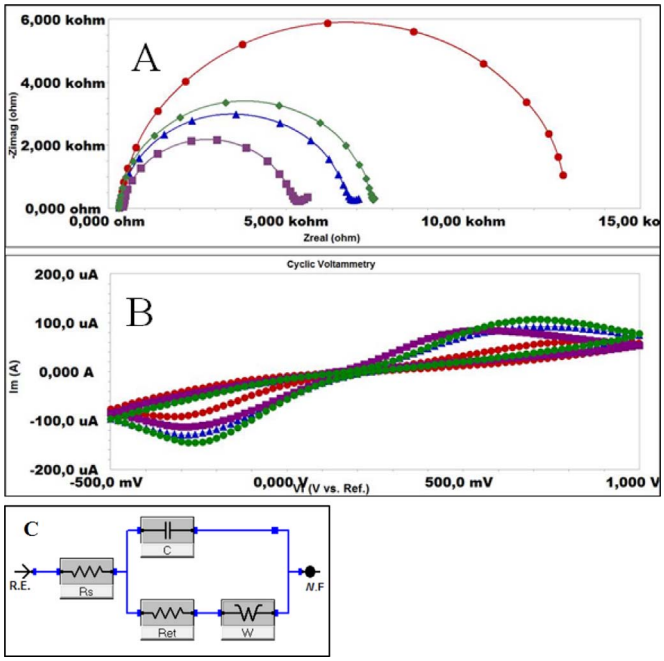

Fig. 1. EIS spectra (A) and CV voltammograms (B) belonging to anti-MAGE-1 immobilization stages. purple [(-■-■-): ITO/OH, red (-•-•-): ITO/OH/3-GOPS, blue (-▲-▲-): ITO/OH/3-GOPS/anti-MAGE, green (-♦-♦-): ITO/OH/3-GOPS /anti-MAGE/BSA], (C) reformed equivalent circuit model for proposed biosensor. (For interpretation of the references to color in this figure legend, the reader is referred to the web version of this article.)

anti-MAGE-1. When the Rct value of the bare ITO surface is compared to Rct value of hydroxyl groups formed on the surface of the ITO electrode, the Rct value of bare ITO was calculated to be 67,690 Ω. This value decreased to 4084 Ω, after the hydroxyl groups were adsorbed on the electrode surface (OH/ITO). The reason for this is that Rct is affected by dielectric and insulator features at the electrode/electrolyte interface. When the electrode surface was covered with 3-GOPS agent used as a SAM material, epoxy groups of 3-GOPS agent pushed the redox probe because of its negative ends and increased the impedance spectrum in relation to the signal, which is dependent on charge transfer resistance (Fig. 1A). In other words, the 3-GOPS agent that contains the epoxy groups did not allow the negative charges of the redox probe to diffuse simply on the electrode surface. In the next step, anti-MAGE-1 antibody was immobilized onto the electrode surface. Comparing the Rct values of 3-GOPS with anti-MAGE-1, with values 36,280 Ω and 9526 Ω respectively, the charge transfer resistance value of anti-MAGE-1 was calculated to be less than 3-GOPS. Efficient diffusion of the redox probe on the electrode surface could be explained by decreased charge transfer resistance as the electrode surface had anti-MAGE-1 immobilized. In the final step of the immobilization process the surface was treated with the blocking agent of BSA solution and it also increased the signal in the impedance spectra. Meanwhile, the increased signal could also be interpreted as the surface of the electrode being insulated by BSA solution.

The anti-MAGE-1 immunosensor was also examined with data obtained from CV voltammograms in the redox solution (5 mM $[Fe(CN)_6]^{3-/4-}$). Traditionally CV, which characterizes the steps of the immunosensor, is a very important device to investigate the electron transfer rate of the modified electrodes. Characteristic anodic-cathodic peak currents belonging to the immunosensor based on anti-MAGE-1 can be clearly seen in Fig. 1B. After the cleaning procedure as previously mentioned, formation of hydroxyl groups on the electrode surfaces provided an increase in the Rct value of redox couple in the anodic-cathodic peak currents. The peak currents clearly decreased by virtue of epoxy groups in the structure of 3-GOPS compound. Both the anodic-cathodic peak currents and the impedance spectra should be coherent with each other to provide evidence of the reliable immobilization of anti-MAGE-1. After the anti-MAGE-1 was covalently bound to the surface, the anodic-cathodic peak currents decreased because of the blocking effect of anti-MAGE-1 on the electron transfer rate. In the final stage of the immobilization process, the surface of the ITO electrode was insulated once more by adding BSA solution, which averted the possibility of causing some disorders in the signal and not being closed effectively with the antibody, and correspondingly the anodic-cathodic peak currents decreased. The conclusion indicates that the anti-MAGE-1 antibody was immobilized on the electrode surface properly and inhibited electron transfer between the redox couple and the ITO electrode. After all immobilization steps the proposed biosensor was ready for use in the determination of anti-MAGE-1.

3.2. Optimization steps of the anti-MAGE-1 immunosensor

It is desirable that the proposed biosensor is sensitive, reproducible and repeatable, and therefore optimization studies are undoubtedly very important. In accordance with this purpose, some necessary optimization steps such as optimization of 3-GOPS concentration,

optimization of anti-MAGE-1 concentration and optimization of anti-MAGE-1 incubation time were completed. Each optimization step was characterized by impedance and voltammetric techniques which are strong tools for studying the measurement stages of immobilization during the immunosensor preparation, determination of anti-MAGE-1 incubation time and anti-MAGE-1 concentration. In the first step of the optimization studies, the ITO-based biosensor was optimized with four different concentrations of 3-GOPS of 0.5%, 1%, 1.5% and 2% (w/v) prepared in toluene solution. Silane ends of 3-GOPS agent, a member of the organosilane family, can be bound with hydroxyl groups formed on the electrode surface after the cleaning procedure. Thus, ITO/OH electrode was modified by 3-GOPS which is a SAM material. Predictably, the optimum concentration to be chosen is extremely important to successfully fabricate the immunosensor and therefore the SAM concentrations were examined in detail. Firstly, the immunosensor was constructed by using 0.5% (w/v) 3-GOPS solution to constitute a conductive surface on the ITO electrode. According to the data obtained with the Rct values in the EIS, a standard curve was drawn. As can be seen from Fig. 1S, the utilized concentration had regular signals but it was not chosen because the signals increased more in higher concentrations of 1%, 1.5% and 2% (w/v). Preparing the immunosensors by using 1%, 1.5% and 2% concentrations of 3-GOPS solution did not exhibit a dramatic signal difference compared to each other. This could be related to the charge transfer resistance which increased by using more concentrated 3-GOPS. In the optimization steps of SAM concentration, the signals at 1.5% concentration and the signals at 2% concentration belonging to 3-GOPS agent, which is the highest concentration, were close together. Therefore, the optimum SAM concentration was chosen as 1.5% (w/v) considering material waste. The standard curves related to these optimizations are given in Fig. 1S, Supplementary material.

To develop stability and sensitivity for the determination of the biosensor, the other important parameter was optimization of anti-MAGE-1 concentration. For this purpose, ITO/OH/3-GOPS electrode was immobilized with four different concentrations of anti-MAGE-1 which are 5.5 ng mL^{-1}, 11 ng mL^{-1}, 55 ng mL^{-1} and 275 ng mL^{-1}. Rct values belonging to these concentrations were calculated as 8770, 9110, 7300 and 5930 Ω, respectively. According to calculated charge transfer resistance values, the lower concentrations were used (5.5 ng mL^{-1}, 11 ng mL^{-1}) because the signals depending on Rct reduced in higher concentrations (55 ng mL^{-1} and 275 ng mL^{-1}). When the signals obtained from these concentrations were compared, it could be seen that 11 ng mL^{-1} anti-MAGE-1 concentration had a regular signal and a higher coefficient of determination (R^2) value than 5.5 ng mL^{-1} concentration. R^2 values (5.5, 11, 55 and 275 ng mL^{-1}) belonging to optimization of anti-MAGE-1 concentrations were 0.9757, 0.9981, 0.976 and 0.9855, respectively. In addition to these, the LOD (limit of detection) values of the immunosensors constructed at these four different concentrations were calculated to confirm that the optimal anti-MAGE1 concentration was chosen. The values (5.5, 11, 55 and 275 fg mL^{-1}) were 5.419, 5.35, 5.41 and 5.39, respectively. Based on these results, 11 ng mL^{-1} concentration, which has the highest Rct, R^2 is close to one and the lowest LOD values, was chosen as optimal anti-MAGE-1 concentration. The standard curves are also given in Fig. 2S. Supplementary material.

After the optimization of anti-MAGE-1 concentration, finally the ITO electrodes were optimized with two different incubation times of 30 min and 60 min. When the anti-MAGE-1 antibody was incubated for 60 min, the signal increased due to an increase in the electron transfer resistance. One of the desirable properties in an ideal biosensor is to provide results in a practical time period. Hence, the electrode surface was incubated for a shorter time (30 min) than 60 min. As can be seen in Fig. 3S. using both incubation times gave very close results to signals in the standard curve. Therefore, because 30 min is sufficient to effectively bind to the electrode surface and also by considering time-saving, it was chosen as an optimal incubation time for the anti-MAGE-1 biosensor.

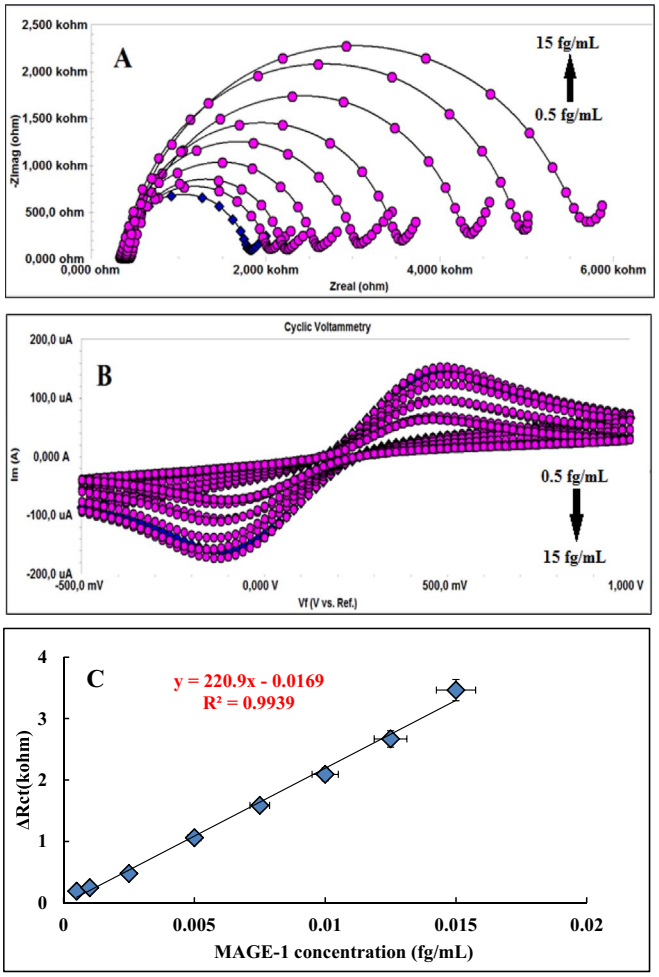

Fig. 2. (A) Impedance spectra (B) cyclic voltammograms of the immunosensor obtained the eight different MAGE-1 concentrations. blue (-◆-◆-): BSA, pink (-•-•-): MAGE-1. (C) MAGE-1 calibration curve obtained by the present anti-MAGE-1 based immunosensor. (For interpretation of the references to color in this figure legend, the reader is referred to the web version of this article.)

3.3. Analytical characterization studies of the anti-MAGE-1 immunosensor

After all immobilization and optimization steps of the proposed immunosensor were completed, a calibration curve that shows the linear detection range of the immunosensor was obtained for anti-MAGE-1 biosensor. The calibration curve of the anti-MAGE immunosensor was calculated by utilizing the equivalent circuit model given in Fig. 1C, below:

$$\Delta R_{ct} = R_{ct}(\text{MAGE}-1) - R_{ct}(\text{BSA})$$

Fig. 2 shows the impedance spectra, CV voltammograms and the calibration curve belonging to the immunosensor. The calibration curve was obtained by using eight different MAGE-1 concentrations to create Nyquist plots in the EIS. The semicircle diameter in the Nyquist plots increased with added MAGE-1 concentrations and the detection range of the immunosensor was determined as 0.5–15 fg/mL (Fig. 2A). In Fig. 2B, when MAGE-1 concentration increased, the peak currents in CV decreased comparatively. Fig. 2C presents a linear graph of the calibration equation of the proposed biosensor. LOD and LOQ (limit of quantification) values of the biosensor, which has a wide detection range, were found to be 0.0035 fg/mL and 0.012 fg/mL, respectively. LOD and LOQ values are calculated with the [$k*S_{blank}/m$]

equation which has k as constant (k is accepted as 3 in LOD and as 10 in LOQ), S_{blank} (standard deviation) and m (slope of the calibration curve).

Repeatability is extremely important parameter for an ideal and sensitive biosensor. To prove the repeatability of the proposed immunosensor, current responses of 20 different disposable ITO electrodes in MAGE-1 concentration at 7.5 fg/mL were measured 20 times, for which the coefficients of variation were calculated to be within 3.5% and standard deviation was obtained as ± 0.26 fg/mL. These calculated values prove the excellent repeatability of the proposed biosensor for detection of MAGE-1 antigen.

The reproducibility of MAGE-1 biosensor was investigated by using 10 different biosensors constructed under the same conditions. Each of the immunosensors demonstrated the same stability in the detection range (0.5–15 fg/mL) for MAGE-1. As a consequence, relative standard deviation (RSD) values, which clarify whether the "regular" standard deviation is a small or large quantity when compared to the mean for the data set, were calculated as 0.21%. The results clearly indicate that the novel immunosensor possesses excellent repeatability, quite good reproducibility, stability and sensitivity for MAGE-1 detection.

The other technique for analytical characterization of the immunosensor is square wave voltammetry (SWV) which is a sensitive and very fast technique for simple reproducible electrochemical data. In our study, SWV was used to support EIS spectra and CV voltammogram results for the immunosensor. For this purpose, BSA and MAGE-1 measurements of eight different ITO electrodes were taken by SWV technique and peak currents belonging to them were obtained. The peak currents obtained by SWV technique showed that the peak currents decreased when the higher MAGE-1 concentration bound onto the surface. The calibration curve and coefficient of determination obtained from these peak currents are given in Fig. 3. The concordance of SWV results with EIS and CV results is an indication that the proposed immunosensor can respond to other electrochemical techniques.

The storage life of the proposed immunosensor was tested for ten weeks. Correspondingly, ten different ITO electrodes with BSA measurements were prepared and then each electrode was measured by adding MAGE-1 concentration in 7.5 fg/mL, weekly. They were stored at +4 °C until use and activity of the proposed immunosensor was calculated at the end of the 10th week. According to the calculated results, activity of the immunosensor reduced from 100% to 88% at the end of the 9th week but the proposed immunosensor did not respond in the 10th week (Fig. 4). The results indicated that the proposed biosensor could be preserved with high activity for a long period of time.

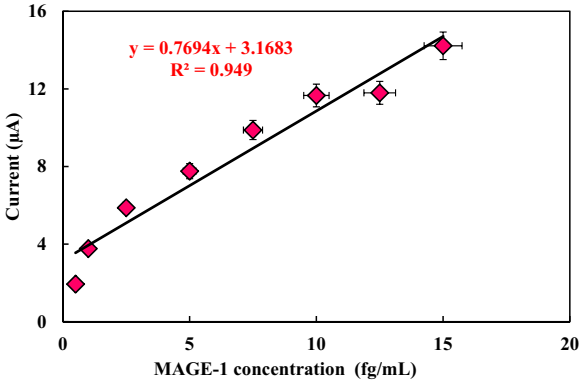

Fig. 3. The calibration curve belonging to MAGE-1 formed by the SWV.

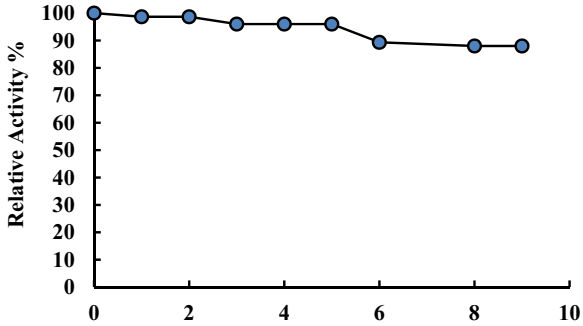

Fig. 4. The storage life of the proposed biosensor for ten weeks.

3.4. Regeneration of the proposed immunosensor

Regeneration is an extremely important process which allows the device to be portable, automated and easy to use [32]. Further, regeneration of the proposed biosensor is a very important point for cost of the study. Regeneration can be considered as a measure of biological activity of the antigen attached to the electrode surface. In this study, after the MAGE-1 concentration in 7.5 fg/mL was incubated onto the disposable ITO electrode for 30 min, the electrode surface was regenerated by treatment with HCl acid (10 mM). This process was performed by immersing the electrode in 150 µL HCl solution for 5 min. Following this, the regenerated surface was incubated with MAGE-1 concentration in 7.5 fg/mL again and in this way the surface of the proposed biosensor was regenerated 5 times. The surface of electrode was broken substantially in the 6th regeneration step. These results showed that the proposed immunosensor preserved 88% of its initial activity at the end of the sixth regeneration step. Undoubtedly, this result is very good for an immunosensor that is expected to be highly stable, repeatable, and low cost.

3.5. Single frequency impedance (SFI) measures and Kramers-Kronig transforms of the immunosensor

Single frequency technique displays the time-dependent changes on the biosensor surface at fixed frequency allowing assessment of the kinetic parameters of antibody-antigen interactions over the measurement [25]. In this technique, impedance measurements were taken at a fixed frequency versus time, therefore the frequency was determined from the Bode plot showing each frequency in the electrochemical impedance spectroscopy. After the frequency was chosen for the SFI, the measurement was taken by using 12.5 pg/mL MAGE-1 concentration during 30 min in 50 mM phosphate buffers (pH 7.0). The results of the SFI measurement showed that between anti-MAGE-1 antibody and MAGE-1 antigen binding could be observed clearly over 30 min (Fig. 5).

Kramer's-Kronig transform provides comprehension of whether the impedance spectra of the proposed immunosensor system are influ-

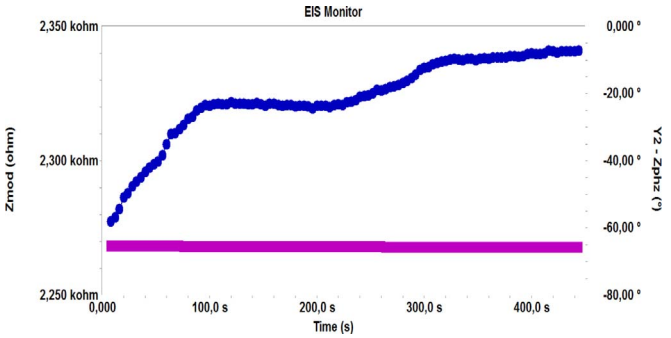

Fig. 5. Single frequency impedance measurement of the proposed immunosensor.

Table 1
The results for Kramer's-Kronig transforms, the sample analysis and comparison of methods used for MAGE-1.

Biosensor surfaces	Goodness of fit values
Kramer's-Kronig transforms performed on different layers of the proposed biosensor	
ITO/OH	1.632
ITO/OH/3-GOPS	2.107
ITO/OH/3-GOPS/ Anti-MAGE-1	3.009
ITO/OH/3-GOPS/ Anti-MAGE-1/BSA	294
ITO/OH/3-GOPS/ Anti-MAGE-1/BSA/ MAGE-1	316.1

Comparison of the results obtained by using ELISA and the proposed biosensor

	ELISA (ng/mL)	Biosensor (ng/mL)	Difference (%)
Sample 1	10.41463	10.75	3.22
Sample 2	21.30894	21.75	2.07
Sample 3	20.14634	20	0.72

enced by the diversity owing to external factors [31,33]. Thanks to this method the electrochemical impedance spectroscopy can be analyzed correctly, and the method also supports stability of the proposed immunosensor. The principle of method is based on the computation of a real section of impedance data by using the imaginative section or computation of the imaginative section by using real section. Accordingly, after the data obtained from Nyquist plots for the immunosensor in EIS were fitted, the potentiostat device gave the goodness of fit values belonging to different biosensor surfaces. The Nyquist plots of Kramer's-Kronig transform and the goodness of fit values for MAGE-1 immunosensor are given in Fig. 4S and Table 1, respectively.

3.6. SEM images of the proposed biosensor

To observe the surface morphology of MAGE-1 immunosensor, SEM images were taken by using a scanning electron microscope. As seen in Fig. 5S, each stage of the proposed biosensor was monitored. In Fig. 5S-A, the bare ITO electrode which has a homogeneous surface was examined. The homogeneous surface was changed after the hydroxyl groups formed on the ITO electrode (in Fig. 5S-B). Moreover, Fig. 5S-C illustrates the SAM layer which formed due to 3-GOPS agent on the surface. When ITO/OH/3-GOPS electrode was treated with anti-MAGE-1 antibody, the surface was more intense than in previous steps in Fig. 5S-D. The surface morphology of ITO/OH/3-GOPS/anti-MAGE-1 electrode after BSA blockage immobilization is seen clearly in Fig. 5S-E. Finally, Fig. 5S-F shows the surface morphology emerging as a result of interaction between anti-MAGE-1 antibody and MAGE-1 antigen.

3.7. Application of the proposed biosensor in ELISA kit and in human serum

In the last step of the characterization studies of the proposed immunosensor, the electrodes were incubated in six different human serum samples diluted to the detection range of the biosensor. The results are given in Table 1. Moreover, the proposed immunosensor was compared to a commercial ELISA (Enzyme-Linked Immuno Sorbent Assay) kit for the same human serum samples. The detection range of MAGE-1 for this commercial kit is in the range of 0.625 ng/mL–40 ng/mL. The comparison of these two techniques is shown in Table 1.

4. Conclusion

In the aimed study, a novel, sensitive and reusability MAGE-1 immunosensor has been developed successfully based on modified ITO electrode. This disposable electrode is advantageous than metal electrode which is like glassy carbon electrode, gold electrode, due to its very cheap. Thanks to carefully the optimization studies which are anti-MAGE-1 concentration and MAGE-1 incubation time, could be constructed a high sensitive and practical MAGE-1 biosensor. The reusable biosensor being prepared without the need for any cross-linking agent due to the 3-GOPS material, has a wide detection range (0.05–15 fg/mL). The human serum study showed that the proposed biosensor could correctly analyze detection of MAGE-1 with low-cost disposable ITO electrodes instead of expensive methods like ELISA testing. Attendantly, it can be expected that this electrochemical immunosensor provided a promising candidate for sensitive detection of MAGE-1 in biological patterns, which may be has good rapport to the applications in cancer biomarker determination. On the other hand, stability, accurate and sensitive of our biosensor system was supported by SWV technique. In this highly sensitive and very fast voltammetric technique were obtained extreme results. Long storage life of the proposed biosensor is remarkable advantage which is particularly a importance in clinical implementations. The 3-GOPS agent and MAGE-1 antigen chosen in the developed biosensor which is a very important detail in terms of the novel of the article, have not been previously used for any immunosensor in the literature. Finally, in this study we was developed the proposed MAGE-1 biosensor which was reusable sensitive, practical, low-cost and wide detection range possesses extreme potential in cancer biomarker diagnosis.

Acknowledgement

We are grateful for the financial supports of this research from The Scientific and Technological Research Council of Turkey (Project number: 113 Z 678)

Appendix A. Supplementary material

Supplementary data associated with this article can be found in the online version at doi:10.1016/j.talanta.2017.03.076.

References

[1] P. van der Bruggen, C. Traversari, P. Chomez, C. Lurquin, E. De Plaen, B. Van den Eynde, A. Knuth, T. Boon, A gene encoding an antigen recognized by cytolytic T lymphocytes on a human melanoma, Science 254 (1991) 1643–1647.
[2] Q. Zhao, O.L. Caballero, A.J. Simpson, R.L. Strausberg, Differential evolution of MAGE genes based on expression pattern and selection pressure, PLoS One 7 (2012) 10.
[3] M. Sang, L. Wang, C. Ding, X. Zhou, B. Wang, Y. Lian, B. Shan, Melanoma-associated antigen genes- an update, Cancer Lett. 302 (2011) 85–90.
[4] P. Chomez, O. De Backer, M. Bertrand, E. De Plaen, T. Boon, S. Lucas, An overview of the MAGE gene family with the identification of all human members of the family, Cancer Res. 61 (2001) 5544–5551.
[5] A.J. Simpson, O.L. Caballero, A. Jungbluth, Y.T. Chen, L.J. Old, Cancer/testis antigens, gametogenesis and cancer, Nat. Rev. Cancer 5 (2005) 615–625.
[6] P.A. Barker, A. Salehi, The MAGE proteins: emerging roles in cell cycle progression, apoptosis and neurogenetic disease, J. Neurosci. Res. 67 (2002) 705–712.
[7] C. Osterlund, V. Tohonen, K.O. Forslund, K. Nordqvist, Mage-b4, a novel melanoma antigen (MAGE) gene specifically expressed during germ cell differentiation, Cancer Res. 60 (2000) 1054–1061.
[8] D.W. Meek, L. Marcar, MAGE-A antigens as targets in tumour therapy, Cancer Lett. 324 (2012) 126–132.
[9] M.J. Scanlan, A.J. Simpson, L.J. Old, The cancer/testis genes: review, standardization and commentary, Cancer Immun. 4 (2004) 1.
[10] L. Bao, K. Dunham, K. Lucas, MAGE-A1, MAGE-A3 and NY-ESO-1 can be upregulated on neuroblastoma cells to facilitate cytotoxic T lymphocyte- mediated tumor cell killing, Cancer Immunol. Immunother. 60 (2011) 1299–1307.
[11] S. Lorenzi, M. Forloni, L. Cifaldi, C. Antonucci, A. Citti, R. Boldrini, M. Pezzullo, A. Castellano, V. Russo, P. Van der Bruggen, P. Giacomini, F. Locatelli, D. Fruci, IRF1 and NF-kB restore MHC class I-restricted tumor antigen processing and presentation to cytotoxic T cells in aggressive neuroblastoma, PLoS One 7 (2012) 1.

[12] T. Ribeiro, C. Baleizao, J. Paulo, Functional films from silica/polymer nanoparticles, Materials 7 (2014) 3881–3900.
[13] Z. Ma, X. Liu, Y. Guan, H. Liu, Synthesis of magnetic silica nanospheres with metal ligands and application in affinity separation of proteins, Colloid Surf. A: Physicochem. Eng. Asp. 275 (2006) 87.
[14] G. Zhang, Q. Cao, N. Li, K. Li, F. Liu, Tris(hydroxymethyl)aminomethane-modified magnetic microspheres for rapid affinity purification of lysozyme, Talanta 83 (2011) 1515.
[15] H. Jenny, M. Fatin, A.D. Nawwa, A.A. Aswan, S. Cordelia, D.X. Sue, P. Magdalena, M.F. Gareth, Colloids Surf. B: Biointerfaces 83 (2011) 83.
[16] K. Li, Z. Zeng, J. Xiong, L. Yan, H. Guoa, S. Liu, Y. Daia, T. Chen, Colloids Surf. A: Physicochem. Eng. Asp. 465 (2015) 113.
[17] X. Dai, R.G. Compton, Direct electrodeposition of gold nanoparticles onto indium tin oxide film coated glass: application to the detection of arsenic(III), Anal. Sci. 22 (2006) 567.
[18] Y.T. Ma, J.W. Di, X. Yan, M.L. Zhao, Zh.J. Lu, Y.F. Tu, Direct electrodeposition of gold nanoparticles on indium tin oxide surface and its application, Biosens. Bioelectron. 24 (2009) 1480.
[19] J. Kariuki, E. Ervin, C. Olafson, Development of a novel low-cost, disposable wooden pencil graphite electrode for use in the determination of antioxidants and other biological compounds, Sensors 15 (2015) 18887.
[20] E. Alipour, M.R. Majidi, A. Saadatirad, S.M. Golabi, A.M. Alizadeh, Simultaneous determination of dopamine and uric acid in biological samples on the pretreated pencil graphite electrode, Electrochim. Acta 91 (2013) 36.
[21] D.W. Wang, F. Li, J.P. Zhao, W.C. Ren, Z.G. Chen, J. Tan, Z.S. Wu, I. Gentle, G.Q. Lu, H.M. Cheng, Fabrication of graphene/polyaniline composite paper via in situ anodic electropolymerization for high-performance flexible electrode, ACS Nano 3 (2009) 1745.
[22] W.H. Cai, T. Lai, H.J. Du, J.S. Ye, Electrochemical determination of ascorbic acid, dopamine and uric acid based on an exfoliated graphite paper electrode: a high performance flexible sensor, Sens. Actuators B 193 (2014) 492.
[23] Y. Altın, M. Taş, İ. Borazan, A. Demir, A. Bedeloğlu, Solution-processed transparent conducting electrodes with graphene, silver nanowires and PEDOT: PSS as alternative to ITO, Surf. Coat. Technol. 302 (2016) 75–81.
[24] L. Fan, X. Kan, Disposable graphite paper based sensor for sensitive simultaneous determination of hydroquinone and catechol, Electrochim. Acta 213 (2016) 504–511.
[25] B. Demirbakan, B. Özcan, Ş.G. Yeşiller, M.K. Sezgintürk, Introducing a new method for evaluation of the interaction between an antigen and an antibody: single frequency impedance analysis for biosensing systems, Talanta 125 (2014) 7–13.
[26] L. Duan, Y. Li, S.S-C, Z. Wan, J. Zhai, Rapid and simultaneous detection of human hepatitis B virus and hepatitis C virus antibodies based on a protein chip assay using nano-gold immunological amplification and silver staining method, BMC Infect. Dis. 5 (2005) 53.
[27] S.P. FitzGerald, J.V. Lamont, R.I. McConnell, E.O. Benchikh, Development of a high throughput automated analyzer using biochip array technology, Clin. Chem. 51 (2005) 1165–1176.
[28] J. Piehler, A. Valiokas, R. Liedberg, G. Gauglitz, A high-density poly(ethylene glycol) polymer brush for immobilization on glass-type surfaces, Biosens. Bioelectron. 15 (2000) 473–481.
[29] G.T. Hermanson, Bioconjugate Techniques, Second Edition, San Diego, 2008.
[30] X.Y. Lin, Y.N. Ni, S. Kokot, An electrochemical DNA-sensor developed with the use of methylene blue as a redox indicator for the detection of DNA damage induced by endocrine-disrupting compounds, Anal. Chim. Acta 867 (2015) 29–37.
[31] B. Özcan, B. Demirbakan, Ş.G. Yeşiller, M.K. Sezgintürk, Introducing a new method for evaluation of the interaction between an antigen and an antibody: single frequency impedance analysis for biosensing systems, Talanta 125 (2014) 7–13.
[32] R. Wang, Y. Xiang, Z. Xiaohong, A reuasble aptamer-based evanescent wave all-fiber biosensor for highly sensitive detection of Ochratoxin A, Biosens. Bioelectron. 66 (2015) 11–18.
[33] B. Özcan, M.K. Sezgintürk, Graphene oxide based electrochemical label free immunosensor for rapid and highly sensitive determination of tumor marker HSP70, Talanta 160 (2016) 367–374.
[34] N. Yanagawa, G. Tamura, H. Oizumi, MAGE expressions madiated by demethylation of MAGE promoters induce progression of non-small cell lung cancer, Anticancer Res. 31 (2011) 171–175.
[35] V. Corbiere, J. Chapiro, V. Stroobant, Antigen spreading contributes to MAGE vaccination-induced regression of melanoma metastases, Cancer Res. 71 (2011) 1253–1262.
[36] A.P. Cogdill, D.T. Frederick, Z.A. Cooper, Targeting the MAGE A3 antigen in pancreatic cancer, Surgery 152 (2012) 13–18.
[37] E.A. Abd-Elsalam, N.A. Ismaeil, Melanoma-associated antigen genes: a new trend to predict the prognosis of breast cancer patients, Med. Oncol. 31 (2014) 285.
[38] A. Bergeron, V. Picard, H. LaRue, High frequency of MAGE-A4 and MAGE-A9 expression in high-risk bladder cancer, Int. J. Cancer 125 (2009) 1365–1371.